Supporting Information

Paper: **Cation diffusion in compacted clay: a pore-scale view**

Authors: Yuankai Yang and Moran Wang*

Department of Engineering Mechanics and CNMM, Tsinghua University, Beijing 100084, China

Pages: S1-S7

Includes: Supporting Figure S1

Supporting Figure S2

Supporting Figure S3

Supporting Table S1

Supporting Table S2

References

* Corresponding author. E-mail address: mrwang@tsinghua.edu.cn

Numerical framework

Benefiting the high efficiency of lattice Boltzmann method (LBM) for parallel computing, the LBM is used as our numerical framework in this study. The corresponding numerical lattice evolution equations for concentration C_i^P and electrical potential ψ^P are shown as [1, 2]:

$$f_{i,\alpha}\left(\boldsymbol{r}+c_{f_i}\delta t_{f_i}\boldsymbol{e}_\alpha,t+\delta t_{f_i}\right)-f_{i,\alpha}\left(\boldsymbol{r},t\right)=-\frac{1}{\tau_{f_i}}\left[f_{i,\alpha}\left(\boldsymbol{r},t\right)-f_{i,\alpha}^{eq}\left(\boldsymbol{r},t\right)\right], \tag{S.2}$$

$$g_\alpha\left(\boldsymbol{r}+c_g\delta t_g\boldsymbol{e}_\alpha,t+\delta t_g\right)-g_\alpha\left(\boldsymbol{r},t\right)=-\frac{1}{\tau_g}\left[g_\alpha\left(\boldsymbol{r},t\right)-g_\alpha^{eq}\left(\boldsymbol{r},t\right)\right]+\omega_\alpha\delta t_g\frac{\rho_e^P}{\varepsilon_r\varepsilon_0}, \tag{S.3}$$

where $f_{i,\alpha}$ and g_α denote the distribution functions for concentration of i^{th} ion and electrical potential, respectively. $\tau_{f_i}=4D_{i,0}\delta t_{f_i}/\delta x^2+0.5$ and $\tau_g=4\delta t_g/\delta x^2+0.5$ are corresponding dimensionless relaxation times. $\boldsymbol{r}$ denotes the position vector, δt corresponding time step, δx lattice size and $\boldsymbol{e}_\alpha$ the discrete velocities where $\alpha=0,1,\mathrm{L}\ ,6$ representing the discretized directions for a 3D seventh speed (D3Q7) scheme. The equilibrium distribution functions for corresponding evolution equations are $f_{i,\alpha}^{eq}=\omega_\alpha C_i^P\left(1-4D_{i,0}\boldsymbol{e}_\alpha ez_i\nabla\psi^P/kTc_{f_i}\right)$ and $g_\alpha^{eq}=\omega_\alpha\psi^P$ respectively, where the distribution coefficients $\omega_{\alpha=0}=1/4$ and $\omega_{\alpha=1\sim6}=1/8$ in D3Q7 system. The concentration and electrical potential are $C_i^P=\sum f_{i,\alpha}$ and $\psi^P=\sum g_\alpha$. For the corresponding boundary conditions of LBM, the conventional bounce-back rule is employed as the zero normal flux boundary condition for ion transport. The constant surface charge density σ_0 boundary condition follows [3]: $g_\alpha\left(\boldsymbol{r},t+\delta t_g\right)-g_\beta\left(\boldsymbol{r},t\right)=\delta t_g\sigma_0/\varepsilon_r\varepsilon_0\delta x$, where the index α

and β is the opposite directions normal to the interface and β is the direction towards wall. The Poisson equation is solved iteratively in the LBM scheme until the electrical potential convergence is reached at each time step of the evolution of ions. In this investigation, the set of coupled ion and electrostatic potential evolution equations in charged clay are solved by the GPU-LBM codes on Tesla-K80 GPU [2, 4-7].

Simulation domain

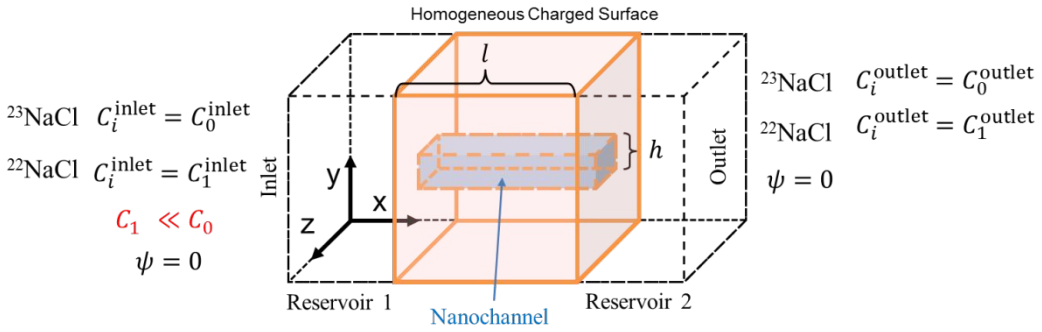

Figure S1 The simulated domain of a nanochannel and corresponding boundary conditions. This domain combines a nanochannel with two reservoirs. The surface of nanochannel is homogeneous charged. The bulk pore solution is 0.01 M ^{23}NaCl electrolyte. h = 3.5 nm is the pore size of nanochannel and l = 9.2 nm the channel length. The tracer's concentration is $C_1^{inlet} = 2.0\times10^{-5}$ M at inlet and $C_1^{outlet} = 1.0\times10^{-5}$ M at outlet.

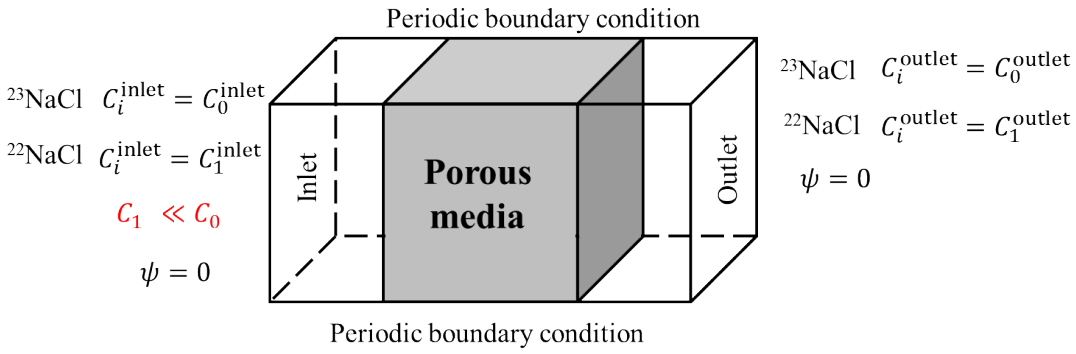

Figure S2 The sketch of the simulation domain: the microstructure of clay is a 192 nm ×192 nm ×192 nm clay and two transition regions. The corresponding boundary conditions are shown in each sides and the bulk concentration. The tracer's concentration is $C_1^{\text{inlet}} = 2.0\times10^{-8}$ M at inlet and $C_1^{\text{outlet}} = 1.0\times10^{-8}$ M at outlet.

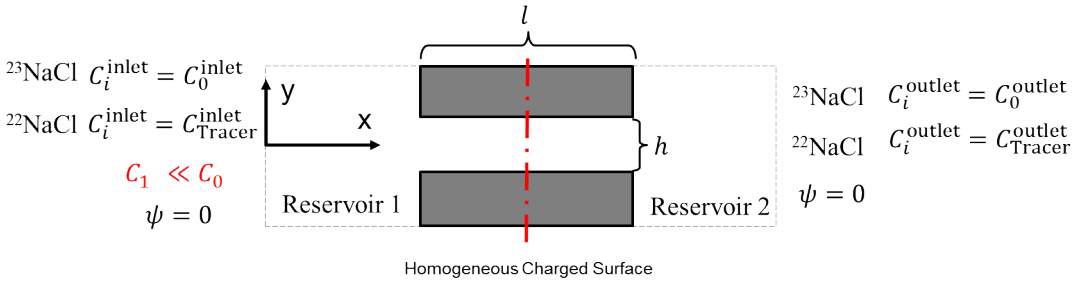

Figure S3 Two-dimensional simulated domain and corresponding boundary conditions. This domain combines a two-dimensional nanochannel with two reservoirs. The surface of nanochannel is homogeneous charged. h = 8 nm is the pore size and l = 48 nm the pore length. The tracer's concentration is $C_{\text{Tracer}}^{\text{inlet}} = 2.0\times10^{-8}$ M at inlet and $C_{\text{Tracer}}^{\text{outlet}} = 1.0\times10^{-8}$ M at outlet.

Reported experiment data

Table S1 Reported experiment data in literature [8-11]. ρ^* is normalized volume charge density and φ the ratio of electrodiffusion of sodium tracer.

Clay	Ionic strength I_S (mol/L)	Dry density ρ_{bd} (kg/m^3)	Porosity θ	CEC (mol/kg)	ρ^*	Effective diffusivity of HTO D_e^{HTO} (×10^{-11} m^2/s)	Effective diffusivity of ^{22}Na$^+$ $D_e^{\text{Na}^+}$ (×10^{-11} m^2/s)	φ	Ref.
Na – M*	0.1	790	0.72	0.82	13	28.00	71.0	0.74	Bestel et al. [11]
	0.1	1020	0.64	0.82	13	18.00	62.0	0.81	
	0.1	1090	0.64	0.82	17	29.00	71.0	0.73	
	0.1	1340	0.52	0.82	34	7.20	45.0	0.89	
	0.1	1620	0.42	0.82	40	3.90	34.0	0.92	
	0.1	1640	0.42	0.82	46	3.60	35.0	0.93	
	1	1320	0.53	0.82	2	3.50	12.0	0.81	
	1	1330	0.53	0.82	2.8	9.10	10.0	0.39	

	1	1680	0.4	0.82	3.8	3.50	5.3	0.56	
	1	1700	0.39	0.82	4.1	3.30	5.0	0.56	
	0.1	1950	0.3	0.82	53.3	1.75	37.0	0.97	Glaus et al. [8] and González Sánchez et al. [9]
	0.5	1950	0.3	0.82	10.7	1.75	8.6	0.86	
	0.7	1950	0.3	0.82	7.61	1.75	5.3	0.78	
	1	1950	0.3	0.82	5.33	1.60	3.8	0.72	
	1	1950	0.3	0.82	5.33	1.60	3.4	0.69	
	0.1	800	0.722	1.08	11.97	6.26	23.3	0.82	
	0.1	800	0.722	1.08	11.97	6.62	24.4	0.82	
	0.5	800	0.722	1.08	2.39	6.84	7.2	0.37	
	0.5	800	0.722	1.08	2.39	8.25	7.6	0.28	
M*	0.1	1900	0.344	0.82	45.2	1.70	38.0	0.97	Glaus et al. [10]
	0.5	1900	0.344	0.82	9.04	1.80	8.4	0.86	
	1	1900	0.344	0.82	4.52	1.90	3.6	0.65	
Illite	0.1	1900	0.296	0.22	14.1	13.00	39.0	0.78	
	0.5	1900	0.296	0.22	2.82	13.00	23.0	0.62	
	1	1900	0.296	0.22	1.41	13.00	13.0	0.34	
Kaolinite	0.1	1900	0.269	0.033	2.33	31.00	32.0	0.36	

*M: montmorillonite;

$\rho^* = \frac{\mathrm{CEC}\rho_{\mathrm{bd}}}{\theta I_S}$;

$\varphi = \frac{D_{e,\mathrm{Na}^+} - D_{0,\mathrm{Na}^+} D_{e,\mathrm{HTO}} / D_{0,\mathrm{HTO}}}{D_{e,\mathrm{Na}^+}}$ with $D_{0,\mathrm{Na}^+} = 1.3\times10^{-9}$ m^2/s and $D_{0,\mathrm{HTO}} = 2.0\times10^{-9}$ m^2/s.

Simulation results

Table S2 As an ion strength gradient applied in two dimensional channel, cationic tracer's total fluxes from pure diffusion term $-D_i\nabla C_i$ and electromigration term $-D_i z_i e C_i \nabla\psi / kT$ on the cross section are calculated. The average concentration $\overline{C} = \left(C_0^{\mathrm{inlet}} + C_0^{\mathrm{outlet}}\right)/2$ equal to 0.05 M. Two surface charge density is considered: -0.01 C/m^2 and -0.005 C/m^2.

Surface charge density (C/m^2)	$\Delta C / \bar{C}$	Concentration gradient of cation tracer $\left(mol/m^4\right)$	Flux from pure diffusion $\left(\times 10^{-7}\ mol/m^2/s\right)$	Flux from electromigration $\left(\times 10^{-7}\ mol/m^2/s\right)$	Sum of Flux $\left(\times 10^{-7}\ mol/m^2/s\right)$	φ	Ξ
-0.01	-1.6	-0.08	0.41	0.54	0.95	0.20	1.34
	-0.8	-0.14	0.69	0.24	0.93	0.19	0.35
	-0.4	-0.16	0.81	0.12	0.92	0.18	0.14
	0	-0.18	0.92	0.00	0.92	0.18	0.00
	0.4	-0.21	1.04	-0.12	0.93	0.18	0.11
	0.8	-0.23	1.17	-0.24	0.93	0.19	0.21
	1.6	-0.30	1.51	-0.56	0.95	0.20	0.37
-0.005	-1.6	-0.12	0.60	0.25	0.85	0.11	0.41
	-0.8	-0.15	0.73	0.11	0.84	0.10	0.15
	-0.4	-0.16	0.78	0.05	0.84	0.10	0.07
	0	-0.17	0.84	0.00	0.84	0.10	0.00
	0.4	-0.18	0.89	-0.05	0.84	0.10	0.06
	0.8	-0.19	0.95	-0.11	0.84	0.10	0.12
	1.6	-0.22	1.10	-0.25	0.85	0.11	0.23

Reference

1. Wang, M.; Pan, N., Predictions of effective physical properties of complex multiphase materials. *Materials Science and Engineering: R: Reports* **2008,** *63*, (1), 1-30.
2. Zhang, L.; Wang, M., Modeling of electrokinetic reactive transport in micropore using a coupled lattice Boltzmann method. *Journal of Geophysical Research: Solid Earth* **2015,** *120*, (5), 2877-2890.
3. Tian, H.; Zhang, L.; Wang, M., Applicability of Donnan equilibrium theory at nanochannel-reservoir interfaces. *J. Colloid Interface Sci.* **2015,** *452*, 78-88.
4. Wang, M.; Wang, J.; Pan, N.; Chen, S., Mesoscopic predictions of the effective thermal conductivity for microscale random porous media. *Physical Review E* **2007,** *75*, (3), 036702.
5. Kuznik, F.; Obrecht, C.; Rusaouen, G.; Roux, J.-J., LBM based flow simulation using GPU computing processor. *Computers & Mathematics with Applications* **2010,** *59*, (7), 2380-2392.
6. Rinaldi, P. R.; Dari, E. A.; Vénere, M. J.; Clausse, A., A Lattice-Boltzmann solver for 3D fluid simulation on GPU. *Simulation Modelling Practice and Theory* **2012,** *25*, 163-171.
7. Obrecht, C.; Kuznik, F.; Tourancheau, B.; Roux, J.-J., Scalable lattice Boltzmann solvers for CUDA GPU clusters. *Parallel Computing* **2013,** *39*, (6-7), 259-270.
8. Glaus, M. A.; Baeyens, B.; Bradbury, M. H.; Jakob, A.; Van Loon, L. R.; Yaroshchuk, A., Diffusion of 22Na and 85Sr in Montmorillonite: Evidence of Interlayer Diffusion Being the Dominant Pathway at High Compaction. *Environ. Sci. Technol.* **2007,** *41*, (2), 478-485.
9. González Sánchez, F.; Van Loon, L. R.; Gimmi, T.; Jakob, A.; Glaus, M. A.; Diamond, L. W., Self-diffusion of water and its dependence on temperature and ionic strength in highly compacted montmorillonite, illite and kaolinite. *Appl. Geochem.* **2008,** *23*, (12), 3840-3851.
10. Glaus, M. A.; Frick, S.; Rossé, R.; Loon, L. R. V., Comparative study of tracer diffusion of HTO, 22Na+ and 36Cl− in compacted kaolinite, illite and montmorillonite. *Geochim. Cosmochim. Acta* **2010,** *74*, (7), 1999-2010.
11. Bestel, M.; Glaus, M. A.; Frick, S.; Gimmi, T.; Juranyi, F.; Van Loon, L. R.; Diamond, L. W., Combined tracer through-diffusion of HTO and 22 Na through Na-montmorillonite with different bulk dry densities. *Appl. Geochem.* **2018,** *93*, 158-166.